ACTIVATED CARBON PREPARED FROM SOFTWOOD LIGNOCELLULOSIC BIOMASS – *OPUNTIA FICUS INDICA* CORDS TO REMOVE AN ANIONIC DYE

AIDA FEKAOUNI,[*] ESIN APAYDIN VAROL,[**] GHANIA HENINI,[***] UMRAN TEZCAN UN[****] and YKHLEF LAIDANI[*]

[*]*Laboratory of Plant Chemistry – Water and Energy, Department of Process Engineering, Faculty of Technology, Hassiba Ben BoualiUniversity of Chlef, Hay Salem, National Road N-19, 0200, Algeria*
[**]*Department of Chemical Engineering, Faculty of Engineering, Eskisehir Technical University, 26555, Eskisehir, Turkey*
[***]*Laboratory of Water and Environment, Department of Process Engineering, Faculty of Technology, Hassiba Ben Bouali University of Chlef, Hay Salem, National Road N-19, 0200, Algeria*
[****]*Department of Environment Engineering, Faculty of Engineering, Eskisehir Technical University, 26555, Eskisehir, Turkey*
✉ *Corresponding author: A. Fekaouni, afekaouni04@gmail.com*

Received July 15, 2023

In this work, lignocellulosic biomass, namely, *Opuntia ficus indica* cords (OFIC), was selected as a renewable resource for the production of activated carbon. The preparation conditions of chemically activated carbon (AC) samples were the following: activation temperature – 600 °C, heating rate – 10 °C min^{-1}, activation time – 60 min, and OFIC/H_3PO_4 impregnation ratio – 1/2. The properties of OFIC and activated carbon were determined by scanning electron microscopy (SEM), Fourier transform infrared spectroscopy (FTIR), thermogravimetric analysis (TGA), Boehm's method, and pHzpc. AC showed heterogeneous surface and acidic characteristics with a pH_{ZPC} of 2.61. OFIC and AC were used as adsorbents to remove the anionic dye Red Bemacid (RB) from aqueous solutions. OFIC was used as a reference for comparison with the prepared AC. The results showed that the experimental data fitted very well with the pseudo-second-order nonlinear model of both adsorbents, with 120 min as equilibrium time and the nonlinear isotherm models of three parameters (Sips and Redlich-Peterson isotherms) were selected as the best fitting ones. The thermodynamic parameters indicated that the adsorption process was spontaneous and endothermic for the AC/RB dye system.

Keywords: Activated carbon, *Opuntia ficus indica* cords, Red Bemacid, adsorption, nonlinear regression

INTRODUCTION

Nowadays, activated carbons have been recognized as a very efficient solution for the treatment of polluted wastewater, such as effluents loaded with textile dyes, which have many detrimental effects on the environment. For this reason, many researchers have investigated various methods to remove dyes from industrial wastewater.[1] Adsorption has proven to be one of the most efficient technologies among other water purification processes.[2]

Many publications in the scientific literature focus on the quality and structure of activated carbon and the factors that influence its structure and adsorption capacity. Biomass plays an important role in activated carbon production. Most lignocellulosic biomass comes from forest waste and agricultural residues, such as *Jatropha curcas* fruit shell,[3] orange peel,[4] prickly pear seed cake,[5] shaddock peel,[6] yellow mombin fruit stones,[7] *Ziziphus mauritiana* nuts,[8] corn cops,[9] eucalyptus, *Delonix regia* pods.[10] Controlling several influencing factors can lead to different properties of activated carbon. One of such factors is biomass quality – lignin-rich biomass provides more activated carbon, while cellulose and hemicelluloses contribute to the production of volatile compounds.[11] In addition to the type of biomass, the type and concentration of

chemical activators are also important. According to previous studies, chemical activation is the best, as it offers several advantages, compared to physical activation methods.[12] Chemical activation has the advantage of producing microporous and mesoporous carbon, whereas physical activation almost exclusively produces microporous activated carbon.[13-14] The most important and commonly used activators are phosphoric acid, zinc chloride, potassium sulfide, magnesium chloride, and alkali metal compounds, such as KOH. All of these chemicals have strong dehydrating effects.[15-16] Researchers impregnated lignocellulosic biomass with these dehydrating agents to inhibit the formation of tar and other liquids and the generation of volatile compounds, thereby promoting the formation of porous structures after the heat treatment.[17] In addition to the biomass and activator nature, activation time and temperature are also among the parameters that have the greatest influence on the structural properties of activated carbon. Many researchers have observed that chemical activation results in an increase in the specific surface area and porosity, due to lower treatment temperatures and shorter treatment times, compared to physical activation.[18-20]

Previous studies aimed at producing activated carbon from OFI under different pyrolysis conditions for application as an adsorbent for the removal of various organic and inorganic wastewaters. Mahi *et al*. used OFI activated with NaOH reinforced by polyaniline for orange-G dye removal from aqueous medium.[21] Wahamu *et al*. studied the production of activated carbon from the cellulosic waste of old OFI cladodes by chemical treatment with H_3PO_4 at a temperature of 450 °C.[22] Chowdhury *et al*. produced biochar and activated biochar from OFI cladodes and leaves as novel adsorbents for the removal of malachite green dye, as well as Cu^{2+} and Ni^{2+} heavy metals.[23]

The purpose of this study was to prepare and characterize activated carbon from raw lignocellulosic biomass (*Opuntia ficus indica* cords), and investigate its ability to adsorb Red Bemacid (RB) dye from aqueous solutions. The activated carbon was produced at a pyrolysis time and temperature of 60 min and 600 °C, respectively, with H_3PO_4 as activator, with the aim to obtain high adsorbent capacity and specific surface area of the adsorbent. The adsorption experiments were carried out using two systems – AC/RB dye and OFIC/RB dye –, for comparison purposes, and the adsorption process was studied as a function of initial concentration of RB dye solution, pH, temperature and adsorbent concentration, to investigate the interaction between RB dye and adsorbent (OFIC and AC). The process was described using nonlinear isotherm models, and thermodynamic parameters were calculated to further understand the adsorption mechanism.

EXPERIMENTAL

Precursor materials

Opuntia ficus indica cladodes were collected from the Chlef region of Algeria. The cords were removed from old cladodes, cleaned and washed with boiling distilled water to remove color and impurities. After that, the cords were dried and crushed to the size of 300 μm. The cords were placed into a 12% NaOH solution, and then washed and dried again.[24] Finally, the amount received was divided into two parts: one was used as a precursor for activated carbon, and the other was bleached with 12% NaOCl, dried, crushed, sieved and rinsed with distilled water. The samples were kept in desiccators until use as adsorbents for the adsorption studies.

Preparation of activated carbon

The activation of lignocellulosic biomass (OFIC) was performed by the phosphoric acid chemical activation method. 100 g of prewashed biomass was impregnated with phosphoric acid. The ratio of biomass to chemicals was: 1/2. The mixed samples were left at room temperature for 24 h and then dried in an oven at 80 °C. Activation was performed in a reactor containing 20 g of impregnated biomass, fitted inside a muffle furnace, equipped with an automatic sensor and programmed to heat the biomass to 600 °C, at a heating rate of 10 °C/min. When the temperature reached the desired value, it was maintained for 60 min, in the presence of a continuous flow of purified nitrogen, at a flow rate of 100 cm^3/min. The reactor was then cooled to room temperature by natural convection. The resulting activated carbon was removed from the reactor and washed with hot distilled water to remove surface chemical reagents, as well as other organic and inorganic residues until a constant pH was reached. The obtained activated carbon was dried and then stored in glass containers for further characterization and adsorption studies.

Characterization of adsorbents

Efficiency is an important property of activated carbon. It is defined as the ratio (R%) of the production weight of activated carbon (m_{AC}) to the dry weight of the precursor (m_0). The expression for mass efficiency is given by the following formula (1):

$$R\% = \left(\frac{m_{AC}}{m_0}\right) \times 100 \quad (1)$$

Moisture analysis was performed on three samples: lignocellulosic biomass (OFIC), impregnated OFIC and activated carbon (AC), using a Precisa Moisture Analyzer, Model XM60. Each sample was tested at a temperature of 150 °C.

The bulk density and real density of the samples were determined. Real density was calculated using an automatic density analyzer (Ultrapyc 1200e). The pH was measured according to ASTM 873-82. Namely, in a small beaker, 0.5 g of each sample (AC and OFIC) was mixed with 20 mL of boiling distilled water using a magnetic stirrer for 15 min. The solution pH was measured with a pH meter.

The zero point charge pH value is defined as the pH value at which the charge on the surface of activated carbon and raw material is zero. In order to determine it, 0.1 g of the sample (AC and OFIC) was placed in a beaker, and 50 mL of 0.01 M NaCl solution was added to it; the pH was adjusted between 2 and 10, by adding NaOH or HCl, and controlled with a pH meter. The solution was stirred for 48 hours and the final pH was measured. pH_{ZPC} is the point at which the curve pH_{final} = f ($pH_{initial}$ intersects the first pH_{final} bisector = f ($pH_{initial}$).

The acidic or basic nature of the activated carbon surface functional groups can be determined using the Boehm method.[25] In order to neutralize acidic and basic groups, 50 mL of four solutions of NaOH, HCl, Na_2CO_3 and $NaHCO_3$, with a concentration of 0.05N, were prepared. 1 g of AC was added to each solution and stirring was continued for 72 hours. After filtration, the alkaline solution was titrated with HCl (0.1N), and the acidic solution was titrated with NaOH (0.1N). The number of sites of acidic or basic functional groups was determined according to following formula (2):

$$n_{geq}(R) = N_0 \times V_0 - N_f \times N_f \quad (2)$$

where N_0V_0 and N_fV_f represent the number of gram equivalents before and after the reaction, respectively, and n_{geq}(R) is the number of gram equivalents reacted.

Thermal analysis was carried out using a Setaram-Labsysevo TGA. Measurements were performed using a 100 µL lidless Al_2O_3 crucible, with 10 ± 0.5 mg sample, heated from 25 °C to 1000 °C at a nitrogen flow rate of 20 mL/min. The samples were also characterized by Fourier transform infrared spectroscopy (FTIR) using a Thermo Nicolet iS10 FTIR spectrometer. The analysis was recorded by scanning between 4000 cm^{-1} and 400 cm^{-1}, with a resolution of 4 cm^{-1} and a scan number of 32. Pellets were prepared from oven-dried KBr and the samples before analysis. Scanning electron microscopy (SEM) and ImageJ software were used to determine the morphology, structure and particle size of the samples prepared.

Red Bemacid adsorption tests

The adsorption of Red Bemacid (RB) dye from aqueous solution was studied using two adsorbents – OFIC and AC – as described below. Solutions containing adsorbate were prepared by dissolving a precise amount of dye in distilled water to give a concentration of 1 g/L. The solution was then diluted to obtain a standard solution containing 20 to 150 mg/L RB dye, and the adsorption experiment was started.

Batch adsorption experiments were performed with different adsorbents (AC and OFIC) on a water bath shaker at 300 rpm, using a series of 100 mL beakers containing 50 mL of known concentrations (30, 50, 70, 100, 120 and 150 mg/L). Experiments were carried out varying the mass of each adsorbent (1 to 10 g/L) (AC and OFIC sizes (dp (mm) ≤ 0.08)), the temperature (25, 35 and 45 °C) and initial pH (2 to 9). The initial pH of the dye solution was adjusted by adding a dilute solution of 0.1N HCl or 0.1N NaOH. In this study, the effect of contact time on adsorption equilibrium was studied in the range from 5 to 300 min. The residual RB dye concentration was determined using a UV-visible spectrophotometer (UV-1800 Shimadzu). The adsorption capacity q_t (mg/g) and dye removal percentage R (%) at time t were calculated by the following Equations (3) and (4):

$$q_t = \frac{(C_0 - C_t)\,V}{m} \quad (3)$$

$$R\,(\%) = \frac{(C_0 - C_t)}{C_0} \cdot 100 \quad (4)$$

where C_0 and C_t (mg/L) are the concentrations of RB dye solution at the initial and time t (min), respectively; V is the adsorbent volume (L), and m is the adsorbent mass (g).

RESULTS AND DISCUSSION

Characterization of adsorbents

The results of the physical and chemical properties of the three samples (raw OFIC biomass, impregnated OFIC and AC) are shown in Tables 1 and 2. As can be seen from the data in Table 1, the mass efficiency of activated carbon prepared with H_3PO_4 is low, less than 40%, which may be caused by the nature of the lignocellulosic biomass, which does not represent a woody plant. *Opuntia ficus indica* cords are characterized by low lignin content and high hemicellulose and cellulose contents. According to the results of Mannai *et al.*,[26] initial *Opuntia ficus indica* had the following composition: 4.8% lignin, 64.5% hemicelluloses and 53.6% cellulose. Lignin is mainly the carbon source, while cellulose and hemicelluloses contribute more to the production of volatile

substances. In the literature, under the same synthesis conditions, activated carbon obtained from cellulose compounds activated by H_3PO_4 had a higher specific surface area than activated carbon obtained from lignin compounds.[27] The pH_{ZPC} of AC and biomass (OFIC) refers to the pH value at which the positive and negative charges on the surface are equal, and the surface charge is zero; $pH<pH_{ZPC}$ means positively charged, and $pH>pH_{ZPC}$ means negatively charged. Raw biomass has a basic sample, while the AC sample has slightly acidic values. Both samples appeared to be consistent with their measured pH and pH_{ZPC} values, as shown in Table 1.

The results for AC surface functional groups, summarized in Table 2, indicate that the values of acidic groups are more important than those of basic groups. This situation could be expected because the lignocellulosic biomass was activated by phosphoric acid, which led to the addition of carboxyl groups. Moreover, the obtained pH_{zpc} and pH values shown in Table 1 also confirmed this.

Table 1
Properties of OFIC, AC, and impregnated OFIC materials

Parameter	OFIC	AC	Impregnated OFIC
pH	9.55	2.23	-
pH_{pzc}	8.07	2.61	-
Moisture content (%)	10.47	8.26	-
Bulk density(g/cm^3)	0.2837	0.3661	0.2873
Real density (g/cm^3)	1.6087	1.6841	1.5945
Average volume(cm^3)	1.2267	0.9746	1.2773
Mass efficiency (%)	-	29.26	-

Table 2
Surface functional groups of AC

Functional groups of AC (meq/g)				
Acidic				Basic
Carboxylic	Lactone	Phenol	Total	Total
0.016	0.0025	0.0165	0.035	0.005

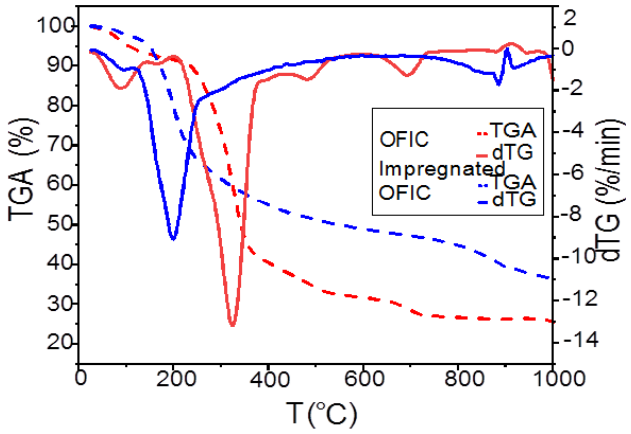

Figure 1: TGA-dTG thermograms of OFIC and impregnated OFIC biomass

Thermo-gravimetric analysis

Thermogravimetric analysis (TGA) and derived thermogravimetric analysis (dTG) allow the study of the thermochemical behavior of biomass (raw and impregnated biomass). The TGA and dTG curves of OFIC impregnated with phosphoric acid H_3PO_4 are shown in Figure 1. In the dTG curve, the first step occurs between 60 °C and 227 °C, with a weight loss of 10% in OFIC. These results can be explained by water loss and decomposition of hemicellulosic materials. The second step is between 243 °C and 361 °C), where the degradation of cellulose and part of hemicelluloses results in a weight loss of 46%, and the final step is between 488 °C and 700 °C), which accounts for 10%. The

weight loss rate can be explained by the decomposition of lignin. Due to the covalent bond between the lignocellulosic structure and the formed phosphate (161 °C to 233 °C), the dTG curve of OFIC impregnated with H_3PO_4 showed thermal stability compared to OFIC, representing cellulose pyrolysis, the weight loss is 25%.[28] According to the literature,[29] the main components of biomass have a characteristic thermal behaviour: hemicelluloses have low thermal stability and their degradation begins at about 200-350 °C; cellulose decomposes in a very narrow range (325-375 °C); and lignin is more thermally stable than cellulose and hemicelluloses, with a larger thermal degradation range (200-800 °C).

FTIR analysis

The FTIR spectra of OFIC biomass and AC, before and after adsorption, and OFIC impregnated with H_3PO_4 were recorded and presented in Figure 2. The FTIR spectrum is obtained in two regions: the fingerprint region at a wavenumber of 1500 cm^{-1} on the right and the chemical functional group region on the left. As shown in Figure 2, OFIC has a higher number of peaks in the fingerprint region. This means there are more chemical functional groups in it, compared to activated carbon (AC). This is clearly due to the lignocellulose content (hemicelluloses, cellulose, and lignin). A large band is observed at 3393 cm^{-1}, which is due to the stretching vibrations of the OH hydroxyl groups (carbonyl, aliphatic and aromatic).[30] OH groups are a major component of lignocellulosic biomass (OFIC), which contains many different polysaccharides, phenolic polymers, and proteins.[31] The band around 2899 cm^{-1} represents aliphatic hydrocarbons C-H. The peak around 1622 cm^{-1} corresponds to C=O stretching vibrations of ketones, aldehydes, carboxyl groups, esters, and anhydrides. The peaks at 1428 cm^{-1}, 1322 cm^{-1}, and 1039 cm^{-1} are assigned to the C-O stretching bands of esters, phenols, and carboxylic acids. The band at 780 cm^{-1} indicates C-Cl due to the use of sodium hypochlorite. According to the literature, the band at 610 cm^{-1} is considered to correspond to an extension of the C-Br band. On the FTIR spectrum of OFIC after adsorption, no significant changes are noted. The type of adsorption may be physical adsorption.

FTIR analysis shows the effect of impregnation and carbonization on the functional groups of the produced activated carbon. The FTIR spectra before and after adsorption of OFIC impregnated with H_3PO_4 and AC are shown in Figure 2. The functional groups (OH, C=O, and C-O) intensity in the spectra of impregnated OFIC and AC decreased and changed, compared to those of OFIC biomass. Furthermore, the peaks appearing at 986 cm^{-1} and 1090 cm^{-1} correspond to aliphatic phosphates (P-O-C).[32] On the FTIR spectrum of AC after adsorption, it may be noted that the hydroxyl group OH disappears – the adsorption type can be regarded as chemical adsorption.

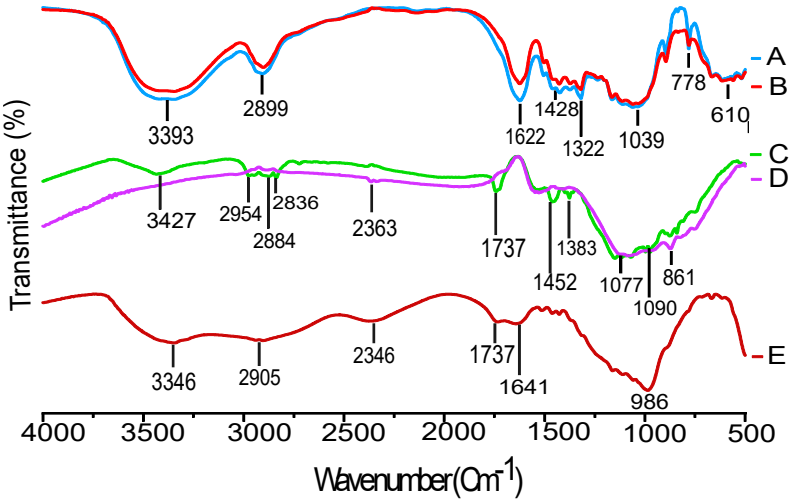

Figure 2: FTIR spectra of (A) OFIC biomass, (B) OFIC after adsorption, (C) AC, (D) AC after adsorption, and (E) impregnated OFIC biomass

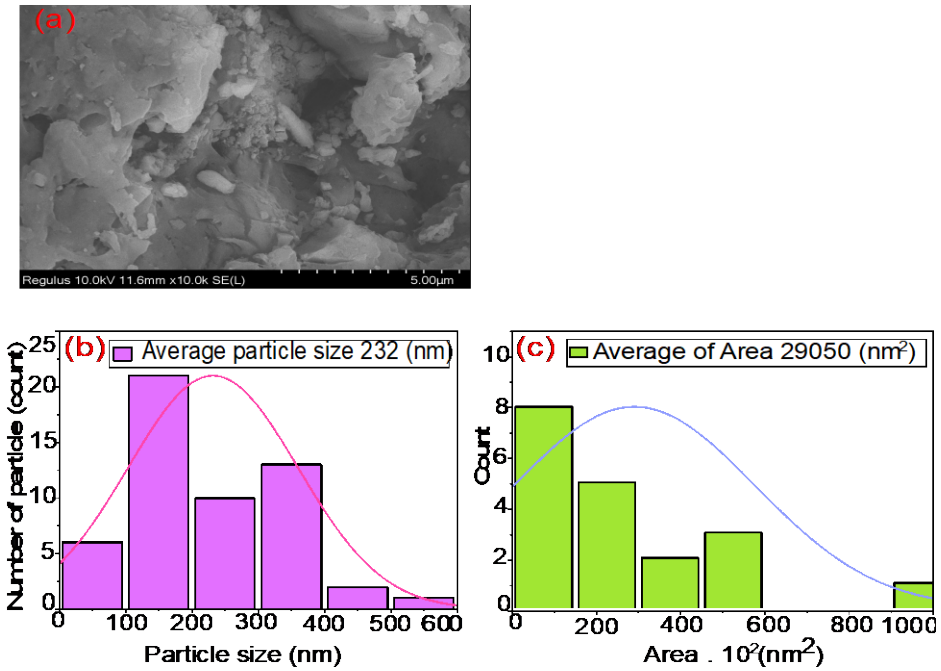

Figure 3: SEM micrograph (a), particle size (b), and area distribution (c) of OFIC biomass

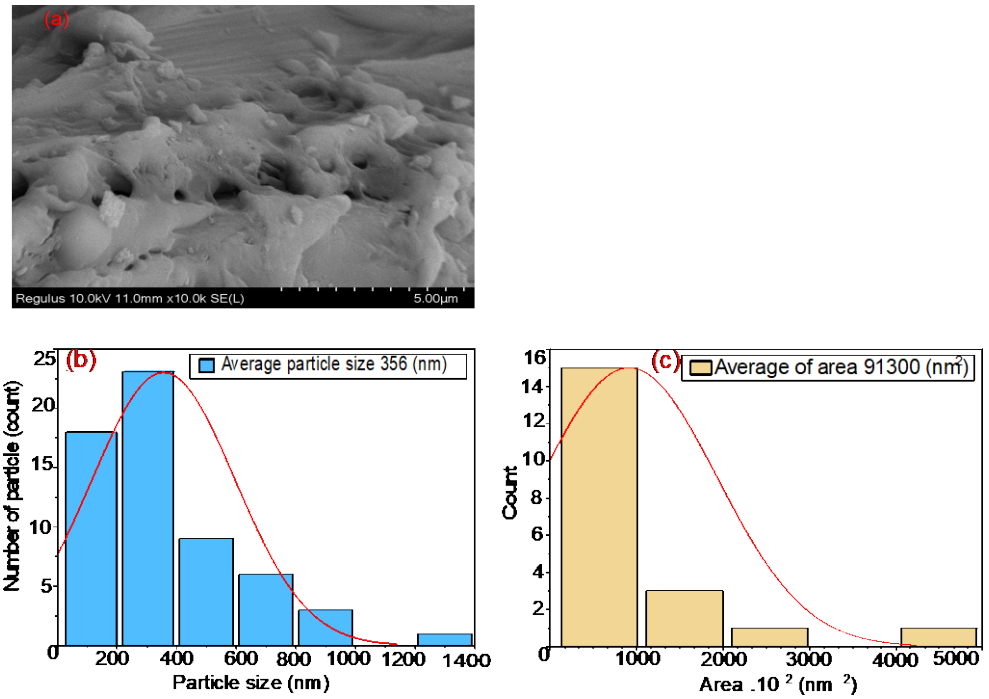

Figure 4: SEM micrograph (a), particle size (b), and area distribution (c) of AC

SEM analysis

Scanning electron microscopy (SEM) was used to observe the external texture and morphology of the samples. SEM images of OFIC biomass and AC are shown in Figures 3 and 4. OFIC biomass exhibits a thick-walled structure and irregular aggregates with low porosity. The SEM image of AC shown in Figure 4 shows a heterogeneous surface, with high porosity and random size distribution. As shown in Figures 3 and 4, the samples (OFIC, AC) differed in surface area and particle size distribution, with average values around 232 nm and 356 nm Comparing the OFIC and AC samples, AC has the most suitable surface structure for adsorption. This is initially caused by the activator (phosphoric acid). This gives the surface of AC stiffness and high porosity. According to the literature, phosphoric acid can react with a number of amorphous polymers

(hemicelluloses, cellulose, and lignin), leading to the formation of microspores, and mesoporous surfaces.[33]

Adsorption RB dye

Effect of contact time on adsorption

The contact time in adsorption determines the equilibrium time and plays an important role in studying kinetic adsorption, as shown in Figure 5. The results indicate that the adsorption capacity of both systems (RB/AC and RB/OFIC) increases rapidly within the first 2 h. After 2 h, the adsorption reached equilibrium. Thus, two stages can be distinguished during the process. The first step, from 5 minutes to 2 h, is called rapid adsorption. This means that RB molecules can be easily guided and transported to the adsorbent surface, because the active sites in this stage are empty, and the RB molecules can be fixed on the surface of the adsorbent. The second step is a slow adsorption process. After 2 h, the amount of adsorbed RB dye did not increase significantly over time. The adsorption rate gradually increased until it became stable. This performance is attributed to the saturation of the active sites of the adsorbent. A comparison of the two adsorption systems is shown in Figure 5. The amount of RB dye adsorbed in the AC adsorbent was larger than that in the lignocellulosic adsorbent. This result indicates that the AC adsorption surface has good adsorption capacity.

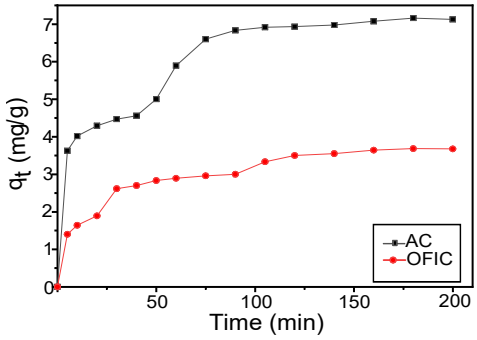

Figure 5: Effect of contact time on RB dye removal onto OFIC and AC adsorbents: $C_{adsorbent}$= 6 g/L, C_0 = 70 mg/L RB dye, T = 25 °C, pH = 5.68, dp (mm) ≤ 0.08 and ω = 300 rpm

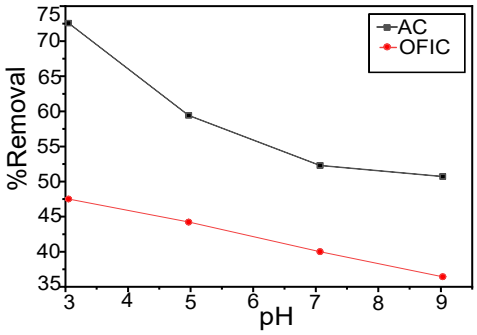

Figure 6: Effect of pH value on the adsorption of RB dye onto OFIC and AC adsorbents; $C_{adsorbents}$ = 6 g/L, C_0 = 70 mg/L RB dye, T = 25 °C and adsorption time 120 min

Influence of pH

By altering the pH of the RB dye solution from 3 to 9, the impact of pH on the adsorption capacity of two adsorbents, AC and OFIC lignocellulosic biomass, was examined. Figure 6 illustrates that the removal percentage of RB dye decreased across the pH range of 3 to 9 for both adsorbents. At a pH of 3, the AC adsorbent exhibited a maximum adsorption rate of 72.57%, while OFIC achieved 47.5% at the same pH level. Also, minimal adsorption occurred at pH = 9, with rates of 50.71% and 36.42%, respectively, and this outcome can be attributed to the slight decline in electrostatic attraction between the negatively charged RB dye and the adsorbent surface. Moreover, increasing the ionic strength of the solution can also reduce electrostatic interactions.[34] The increase in the concentration of H^+, OH^- and other ions is a direct result of the adsorption process. However, this increase eventually hinders the effectiveness of the adsorption process. Additionally, a high pH level causes the concentration of OH^- ions to increase in the solution, potentially leading to electrostatic repulsion with the surface adsorbents when reacting with the anionic RB dye. It has been found that a pH value of 3 is the optimal condition for the adsorption of RB dye onto the mentioned adsorbents. This finding aligns with the majority of previous research studies.[35,36]

Effect of initial concentration RB dye

The impact of varying concentrations of RB dye on the adsorption capacity of two different adsorbents, AC and OFIC lignocellulosic biomass, was examined across a range of concentrations (30, 50, 70, 100, 120, and 150 mg/L dye per liter of solution). The study also involved comparing different initial dye concentrations and types of adsorbents. All tests were conducted at pH = 3 and a temperature of 25 °C.

The results for the adsorption onto AC and OFIC of different RB concentrations are illustrated in Figure 7. The data reveal that the adsorption capacity towards RB dye increases as the initial concentration of RB dye increases. Specifically, when the dye concentration increased from 30 mg/L to 150 mg/L, the adsorption capacities of AC and OFIC increased from 3.52 mg/g to 8.48 mg/g, and from 1.61 mg/g to 7.29 mg/g, respectively. These enhancements in adsorption capacity can be attributed to the migration of RB dye ions towards the interface between the aqueous solution and the adsorbent surface (from high concentration to low concentration), resulting in their immobilization on the adsorbent surface and reduced transport resistance and residence time.[37] Notably, the degree of RB dye adsorption on the AC adsorbent was higher compared to that onto the OFIC biomass adsorbent, a trend that has been reported in the literature as well.[38]

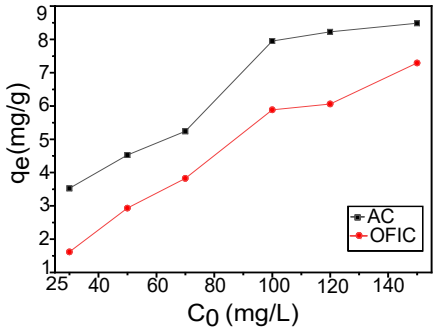

Figure 7: Effect of initial RB concentration on adsorption capacity: pH = 3, $C_{adsorbents}$ = 6 g/L, adsorption time = 120 min, T = 25 °C, dp (mm) ≤ 0.08 and ω = 300 rpm

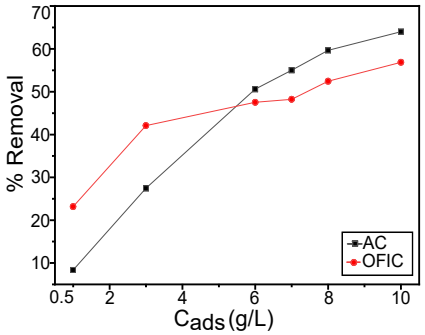

Figure 8: Effect of adsorbent concentration on RB dye removal by OFIC and AC adsorbents: C_0 = 70 mg/L RB dye, pH = 3, adsorption time = 120 min, and T = 25 °C

Effect of adsorbent dose

The RB dye removal percentage is depicted in Figure 8, showing the relationship between adsorbent dosage and removal percentage for both adsorbents (AC and OFIC). It is evident from Figure 8 that as the concentration of the adsorbent increases, the percentage of RB dye removal also increases. This observation is supported by several other researchers.[39,40] The RB dye removal percentage ranged from 8.35%, when 1 g of AC was used per 1 L of RB dye solution, to 64%, when 10 g of AC was used per 1 L of RB dye solution. This can be attributed to the fact that an increase in the amount of adsorbent leads to an increase in the number of available sites for dye adsorption. Also, even when the same amounts of AC and OFIC adsorbents were used for RB dye treatment, there is a variation in the RB dye removal percentage by the two adsorbents. One possible explanation for this may be the difference in the number of available sites for adsorption. Additionally, the adsorption capacity of AC is influenced by the volume and concentration of the RB dye solution, while the OFIC biomass has its limitations, as depicted in Figure 8.

Effect of temperature

Temperature is another important factor in adsorption studies; it plays a role in the adsorption mechanism, controlling molecular motion behavior, and is useful in determining thermodynamic parameters. Figure 9 shows the experimental results of the adsorption of RB dye onto the two adsorbents when the temperature was varied (25, 35, and 45 °C) at different dye concentrations (30-150 mg/L). It can be noticed that, as the temperature of the AC adsorbent increases, the adsorption capacity decreases. These results indicate that the adsorption of RB onto AC is endothermic, whereas the adsorption of RB onto OFIC biomass is exothermic, as shown in Figure 9 (a and b). In this case, this difference may be explained by the deformation and changes in the structural surface of OFIC lignocellulosic biomass at high temperatures. As a result, the interaction between RB dye and OFIC biomass is weaker, leading to desorption of RB dye from the solution interface. In contrast, the interaction between RB dye and activated carbon (AC) becomes stronger at higher temperatures. These findings agree with those of other researchers.[41]

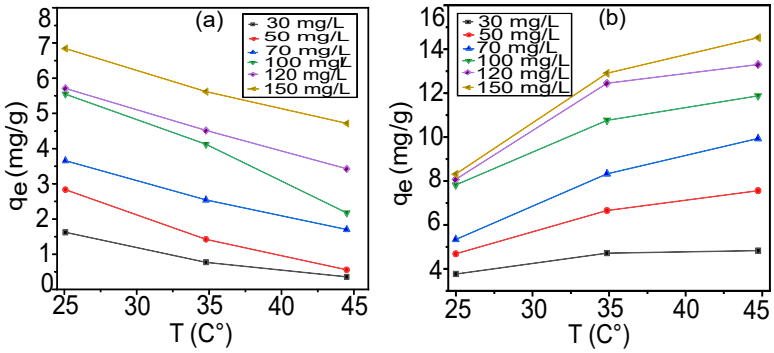

Figure 9: Effect of temperature on RB dye removal by OFIC (a), and AC adsorbent (b): $C_{adsorbent}$ = 6 g/L, adsorption time = 120 min, pH = 3

Adsorption kinetics

In the literature, two well-known models have been used to study the adsorption mechanism and molecular motion behavior: the pseudo-first-order model (Eq. 5) and the pseudo-second-order model (Eq. 6). Using these models, we can estimate the adsorbed amount of RB dye on both adsorbents. Dissolved substances are transferred from the liquid phase to the solid phase. The experimental data were fit to the model equation through nonlinear regression, as follows:[42,43]

$$q_t = q_e\left(1 - exp(-k_1 t)\right) \quad (5)$$

$$q_t = \frac{t}{\left((1/k_2 q_e^2)+(t/q_e)\right)} \quad (6)$$

where q_e is the amount of dye adsorbed at equilibrium (mg/g), q_t (mg/g) is the amount of dye adsorbed at time t, k_1 is the first-order rate constant (min^{-1}), and k_2 is the rate of second-order pseudo-adsorption constant (g/mg min), t is adsorption time (min).

The adsorption kinetic data for the examined adsorbents are shown in Figure 10. Table 3 summarizes all the kinetic parameters obtained experimentally, determined using the nonlinear method, by the OriginLab software. It can be seen from the results that the correlation coefficient and χ^2 value of the pseudo-second-order kinetic model are greater than those of the pseudo-first-order kinetic model, indicating that the pseudo-second-order kinetic model is the most suitable model to describe the adsorption system. These results are similar to those of other researchers.[44,45]

Adsorption isotherms

To study the adsorption of Red Bemacid onto AC and OFIC biomass, three two-parameter models, *i.e.* the Langmuir model, the Freundlich model and the Dubinin-Radushkevich isotherm, and two three-parameter isotherm models (Sips and Redlich-Peterson) were used. Table 4 summarizes the nonlinear regression equations for the selected isotherm models. The purpose of the adsorption isotherm studies has been to understand the adsorption mechanism and describe the adsorption phenomenon.

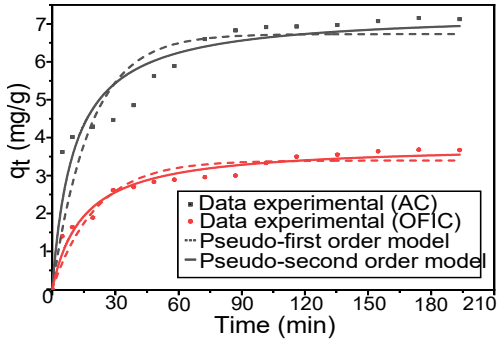

Figure 10: Nonlinear kinetic models of RB adsorption onto AC and OFIC biomass

Table 3
Kinetic parameters of RB dye removal by OFIC and AC

Adsorbent	AC	OFIC
$q_{e,exp}$ (mg/g)	6.933	3.5
Pseudo-first-order model		
$q_{e,cal}$ (mg/g)	6.73322 ± 0.28071	3.39806 ± 0.11261
k_1 (min^{-1})	0.05374 ± 0.0109	0.04625 ± 0.00692
R^2	0.83853	0.91509
χ^2	0.64774	0.09424
Pseudo-second-order model		
$q_{e,cal}$ (mg/g)	7.31758 ± 0.28473	3.82266 ± 0.11578
k_2 (g/mg.min)	0.01276 ± 0.00324	0.01712 ± 0.00298
R^2	0.9197	0.96448
χ^2	0.32214	0.03943

Table 4
Two- and three-parameter isothermal models

Models Non-linear equation		Constants	Refs.
Isotherm models with two parameters			
Langmuir $q_e = (K_L C_e)/(1 + K_L C_e)$ $R_L = 1/(1 + K_L C_0)$	(7) (8)	q_m K_L R_L	Chen *et al*.[46]
Freundlich $q_e = K_F C_e^{1/n}$	(9)	K_F n_F	Khayyun *et al*.[47]
Dubinin-Radushkevich (D-R) $q_e = q_D \exp(-\beta\varepsilon^2)$ $\varepsilon = RT\ln(1 + (1/C_e))$ $E = (1/\sqrt{2\beta})$	(10) (11) (12)	q_D β E	Hu *et al*.[48]
Isotherm models with three parameters			
Sips $q_e = (q_s b_s C_e^{1/n_s}) / (1 + b_s C_e^{1/n_s})$	(13)	q_s b_s n_s	Belhachemi *et al*.[49]
Redlich-Peterson(R-P) $q_e = (K_{RP} C_e)/(1 + \alpha_{RP} C_e^{\beta})$	(14)	K_{RP} α_{RP} β	Li *et al*.[50]

where q_e – the amount of dye adsorbed per unit mass of adsorbent (mg/g), C_e – the equilibrium concentration of dye in the solution (mg/L), K_L – the Langmuir constant (L/mg) and q_m – the maximum adsorption capacity (mg/g), K_F (mg $g^{-1}(Lmg)^{-(1/nF)}$) – the Freundlich constant, ($1/n_F$) – the heterogeneity factor, related to the capacity and the biosorption intensity, q_D (mg/g) – adsorption capacity of the D-R model, β – activity coefficient pertinent to mean adsorption energy, ε – Polanyi potential, qs (mg/g) – adsorption capacity of the Sips model, bs – Sips isotherm model constant (L/g), K_{RP} – adsorption capacity of R-P models, a_{RP} – constant related to adsorption energy of adsorption, β (between 0 and 1) are empirical constants

Well-known two-parameter models (Langmuir, Freundlich, and Dubinin-Radushkevich (D-R)) and three-parameter models (Sips, Redlich-Peterson) were used to estimate experimental RB dye adsorption isotherms and describe the contaminant-adsorbent relationships for the different systems (RB/AC) and (RB/OFIC). Adsorption data from the two previous systems at different temperatures (25 °C, 35 °C, and 45 °C) were fitted by a nonlinear model using the OriginLab version 9.55.

The values of the isotherm constants R^2 (correlation coefficient) and χ^2 chi-square are

listed in Table 5. In addition, the data predicted by the mentioned isotherm models are shown in Figures 11 and 12. The chi-square χ^2 of the two systems (RB dye/AC) and (RB dye/OFIC) at different temperatures (25 °C, 35 °C and 45 °C) corresponds to the value of the correlation coefficient R^2. It can be seen that the Sips model and the Redlich-Peterson model are the most suitable to describe the adsorption equilibrium, and the correlation coefficients of the two systems are relatively high ($R_S^2 = 0.9502$, $R_{RP}^2 = 0.9503$) and ($R_S^2 = 0.9799, R_{RP}^2 = 0.9760$), respectively. These results indicate that competition exists between monolayer and multilayer interactions in both adsorption systems. In the literature, the Redlich-Peterson isotherm is referred to as a combination of the Langmuir and Freundlich isotherms, describing an adsorption mechanism that does not follow an ideal monolayer interaction.[51,52] Therefore, the Sips isotherm is used to predict heterogeneous adsorption systems (RB/AC) and the heterogeneity factor values of (bs) at different temperatures (25 °C, 35 °C and 45 °C) are (1.8914, 2.1420 and 1.2976), indicating that the adsorbent has uniform binding sites. For the adsorption system (RB/OFIC), the values (0.6436, 0.3836 and 0.4920) indicate heterogeneous adsorbents.

Furthermore, Langmuir's separation factor (R_L) allowed confirming the favorability of the adsorption process for both systems.[53] R_L is related to the initial concentration of RB dye at different temperatures, as shown in Figure 13. The separation factor decreases with the increase in the initial concentration of RB dye, indicating that the adsorption of RB dye on AC increases with the increase of the initial concentration of RB dye. Furthermore, the R_L values are between 0 and 1, indicating that the adsorption system (RB dye/AC) is favorable at different temperatures and at all RB dye initial concentrations. Although the adsorption system (RB dye/OFIC) gives the same results as the system (RB dye/AC) at a temperature of 25 °C, when the temperature reached 35 °C and 45 °C, R_L is close to 1, showing unfavorable (linear) adsorption for the adsorption system RB dye/OFIC.

Also, as shown in Table 5, the Dubinin-Radushkevich isotherm model can provide information on the type of adsorption for adsorption energy (E) values below 8 Kj/mol. The results for RB/OFIC suggest that the adsorption is a physical process, being limited by certain operating conditions, and more efficient at low temperatures. In contrast, the adsorption system RB dye/AC is more suitable for higher temperatures.

Table 5
Parameters of nonlinear adsorption isotherms for RB dye on OFIC biomass and AC

Isotherm models with two parameters						
	Activated carbon (AC)			OFIC biomass		
	25 °C	35 °C	45 °C	25 °C	35 °C	45 °C
			Langmuir			
q_m	11.076 ± 1.757	15.695 ± 1.655	15.635 ± 0.539	21.893 ± 7.962	8844.89 ± 3.76×10^6	21396.26 ± 7.85×10^6
K_L	0.0352 ± 0.015	0.0824 ± 0.0289	0.2240 ± 0.0317	0.0048 ± 0.0023	5.80×10^{-5} ± 0.0024	1.55×10^{-6} ± 0.0057
R^2	0.8715	0.9197	0.9809	0.9704	0.9397	0.8016
χ^2	0.7441	1.2915	0.3792	0.1726	0.3185	0.8290
			Freundlich			
K_F	1.34732 ± 0.4462	3.1141 ± 0.456	4.9864 ± 0.566	0.1869 ± 0.0784	0.0194 ± 0.0139	3.29×10^{-4} ± 4.15×10^{-4}
N	0.4125 ± 0.0813	0.3581± 0.0404	0.2816 ± 0.033	0.7919 ± 0.0967	1.2182 ± 0.1595	2.0105 ± 0.2712
R^2	0.8956	0.9657	0.9588	0.9608	0.9618	0.9696
χ^2	0.6046	0.5512	0.8193	0.2281	0.2017	0.1270
			Dubinin-Radushkevick (D-R)			
E	0.0762	0.0763	0.2523	0.0226	0.0131	0.0085
q_D	7.3823 ± 0.7941	12.807± 1.6365	13.2341 ± 0.9128	7.238 ± 0.597	7.135 ± 0.489	7.356 ± 1.482
B	85.9917 ±	85.804 ±	7.8560 ±	975.666 ±	2897.465 ±	6892.028 ±

	50.370	50.65	2.5400	238.990	395.123	1892.196
R^2	0.5815	0.5898	0.8478	0.91406	0.97601	0.93113
χ^2	2.4230	6.5946	3.0270	0.5005	0.12677	0.2877
Isotherm models with three parameters						
Sips						
q_s	28.840 ± 115.315	41.461± 73.521	17.428 ± 2.472	10.137 ± 3.171	7.424 ± 1.283	258.499 ± 11830.80
b_s	0.0392 ± 0.1207	0.0708 ± 0.114	0.250 ± 0.039	0.0018 ± 0.0022	1.63×10^{-5} ± 2.76×10^{-5}	1.16×10^{-6} ± 4.85×10^{-5}
n_s	1.891 ± 2.133	2.1420 ± 1.161	1.297 ± 0.344	0.6436 ± 0.1921	0.3836 ± 0.0720	0.492 ± 0.275
R^2	0.8972	0.9681	0.9855	0.9801	0.990	0.9696
χ^2	0.7934	0.6844	0.3847	0.1543	0.070	0.1694
Redlich-Peterson						
K_{RP}	60.596 ± 13452.26	24.325 ± 203.04	4.909 ± 1.596	0.0892 ± 0.0117	0.0542 ± 0.0035	0.397 ± 8.126
β_{RP}	0.589 ± 0.386	0.656 ± 0.131	0.894 ± 0.069	2.818 ± 3.211	-3.532 ± 2.010	-1.093 ±1.898
α_{RP}	44.5835 ± 10036.31	7.3178± 65.510	0.4771 ± 0.2826	6.135×10^{-7} ± 9.60×10^{-6}	173019.04 ± 1.265×10^{6}	1613.795 ± 22715.21
R^2	0.8956	0.9659	0.9895	0.9775	0.9810	0.9696
χ^2	0.8061	0.7318	0.2777	0.1749	0.1339	0.1693

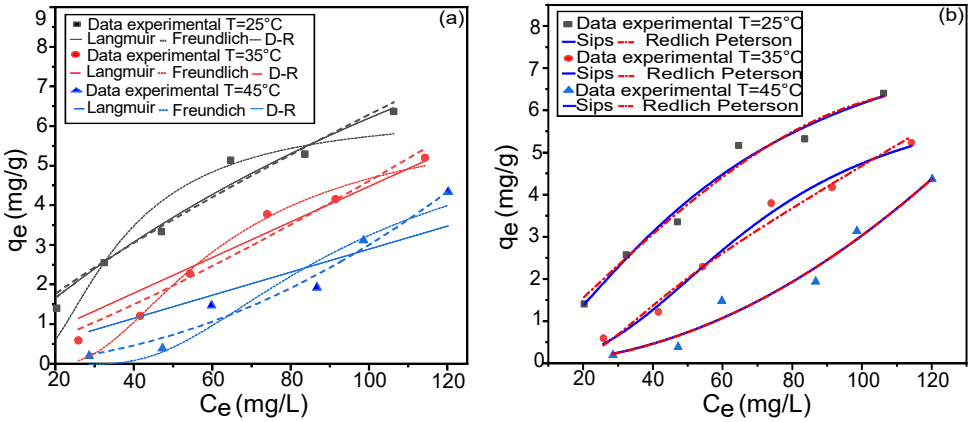

Figure 11: Plots of two-parameter (a), and three-parameter (b) nonlinear isotherms for RB dye adsorption onto OFIC biomass

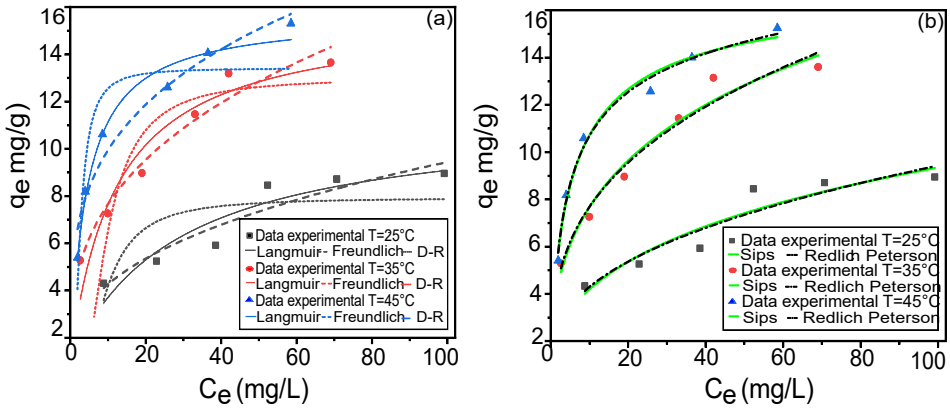

Figure 12: Plots of two-parameter (a), and three-parameter (b) nonlinear isotherms for RB dye adsorption onto AC

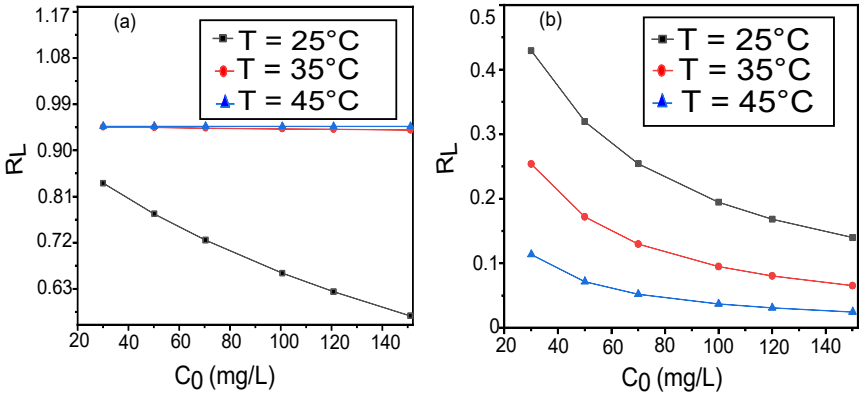

Figure 13: Plots of R_L as a function of initial RB dye concentration at various temperatures for OFIC biomass (a), and AC (b)

Table 6
Comparison of maximum adsorption capacity at optimal parameters for different activated carbon absorbents towards dyes

Precursor/ activation agent	Adsorbate	Optimal parameters				pH_{pzc}	qe (mg/g)	Refs.
		pH	$[dye]_0$ (mg/L)	t (min)	$C_{adsorbent}$ (g/L)			
Hazelnut husk/ $ZnCl_2$	Methylene Blue (MB)	7	800	120	0.5	5.50	476.2	Karaçetin *et al.*[54]
Black cardamom/KOH	Congo Red (CR)	6	100	120	0.4	7.54	69.93	Aftab *et al.*[55]
Persea americana nuts/H_3PO_4	Basic Blue 41 (BB41)	/	125	120	0.6	/	625	Regti *et al.*[56]
Corncob/ H_3PO_4	Methylene Blue (MB)	8	50	120	5	7.4	28.65	El-Sayed *et al.*[57]
Pomegranate peel/HCl	Aniline Blue (AB)	4	30	50	2	7.92	27.322	Usman *et al.*[58]
Opuntia ficus indica cords/H_3PO_4	Red Bemacid (RB)	3	70	120	6	2.61	15.635	Present work

Table 6 shows the maximum adsorption capacity (q_{max}) recorded under the optimal parameters for RB dye adsorption onto AC, compared to the data available in the literature for other AC adsorbents. Compared with other activated carbons reported in the literature, the activated carbon prepared in this study has quite adequate adsorption capacity, considering the initial concentration of dye and the amount of adsorbent.

Adsorption thermodynamics

The measurement of thermodynamic parameters requires understanding of the type of adsorption, whether it is physical adsorption or chemical adsorption, whether it is an exothermic or endothermic phenomenon, including these parameters: change in Gibbs free energy, ΔG^0, enthalpy ΔH^0, and entropy ΔS^0. The thermodynamic parameters were calculated from Equations (15) and (16):[59]

$$\Delta G^0 = -R\,T\,Ln\,(K_d) \quad (15)$$

$$\Delta G^0 = \Delta H^0 - T\Delta S^0 \quad (16)$$

where $K_d = q_e/C_e$ is the distribution coefficient, R is the gas constant (8.314 J/mol K), and T is the absolute temperature.

Equation (16) can be written as follows:[60]

$$Ln\,(\rho\,K_d) = \frac{\Delta S^0}{R} - \frac{\Delta H^0}{R}\cdot\frac{1}{T} = -\frac{\Delta G^0}{R}\cdot\frac{1}{T} \quad (17)$$

where ρ is the density of water (g/L), the values of ΔH^0 and ΔS^0 can be determined from the slope and intercept of the plot between Ln (ρKd) vs (1/T).

Thermodynamic parameters were calculated using Equation (17), as shown in Figure 15. The values of ΔG^0, ΔH^0, and ΔS^0 for the adsorption of RB dye onto lignocellulosic OFIC and AC at

different temperatures (298, 308, and 313 K), with various initial concentrations of RB dye are given in Table 7.

Table 7
Thermodynamic parameters for RB dye adsorption onto OFIC and AC

C_0 (mg/L)	T (K)	ΔH^0 (kJ/mol)	ΔS^0 (kJ/mol.K)	ΔG^0 (kJ/mol)
OFIC biomass				
50	298	-8.7849	-0.2568	67.7683
	308			70.3372
	318			72.9061
70	298	-4.1375	-0.1022	26.3240
	308			27.3462
	318			28.3684
120	298	-2.7214	-0.0556	13.8610
	308			14.4175
	318			14.9740
150	298	-1.9915	-0.0317	7.4577
	308			7.7748
	318			8.0919
Activated carbon (AC)				
50	298	8.9461	0.34430	-93.6553
	308			-97.0983
	318			-100.54
70	298	8.6282	0.3297	-89.6253
	308			-92.9224
	318			-96.2195
120	298	6.5388	0.2567	-69.9667
	308			-72.5340
	318			-75.1013
150	298	5.4426	0.2172	-59.2829
	308			-61.4549
	318			-63.6269

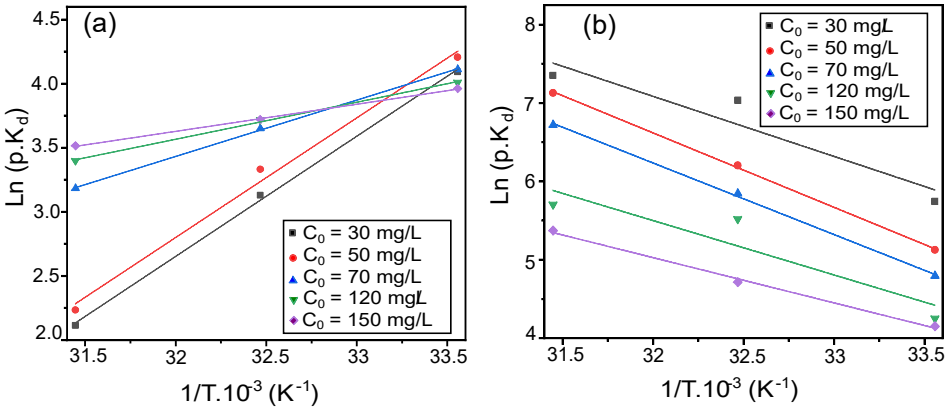

Figure 14: Van't Hoff equation to determine the thermodynamic parameters of adsorption systems OFIC/RB dye (a), and AC/RB dye (b)

The results are shown in Table 7 and Figure 14. It is observed that the value of ΔG^0 is positive and decreases with increasing initial dye concentration for the OFIC/RB system. These results mean that the adsorption phenomenon is not spontaneous. The ΔG^0 values obtained for this system ranged from 20 to 40 kJ/mol, indicating physical adsorption. The free energy change value indicates chemical adsorption when the RB dye concentration is 50 mg/L, and the negative ΔH^0 value indicates that the adsorption type is exothermic. The negative ΔS^0

values at different initial concentrations demonstrate a reduction of randomness for the OFIC/RB adsorption system.

In contrast, the ΔG^0 value for the adsorption system AC/RB was negative and greater than 40 kJ/mol, indicating that the adsorption process is a physical, spontaneous phenomenon. ΔH^0 was positive for all initial concentrations, confirming that the adsorption process is endothermic. Positive values of ΔS^0 indicate increased randomness of the system (AC/RB). Therefore, the adsorption is favorable and there is an affinity between the AC adsorbent and the RB dye adsorbate. The same phenomenon was previously observed during the adsorption of methyl orange on Acacia wood activated carbon (AMW-AC).[61,62]

CONCLUSION

In this study, activated carbon was prepared using *Opuntia ficus indica* cords as raw material and chemical activation was performed using the H_3PO_4 agent. The obtained activated carbon was used as an adsorbent to remove Bemacid Red dye from aqueous solution. The results demonstrated that the AC adsorbent was more efficient than the raw biomass, and was not limited by the operating conditions used in the study. The adsorption process corresponded to the pseudo-second-order model for both adsorbents. The three-parameter fitting nonlinear models (Sips, Redlich-Peterson) were found more suitable than the two-parameter nonlinear fitting models (Langmuir, Freudlich and Dubinin-Radushkevich) for describing the adsorption process for the adsorption systems AC/RB and OFIC/RB. For the system AC/RB, the adsorption process is an endothermic process, while for OFIC/RB, it is an exothermic process. The type of raw material and the activation agent are parameters that influence the effectiveness of the adsorption process. The initial concentration of the RB dye solution affects the thermodynamic parameters. The results of this study demonstrate that OFIC can serve as a cost-effective alternative for the production of activated carbon, using phosphoric acid as activating agent, to obtain an efficient removal of anionic dyes from aqueous solutions.

ACKNOWLEDGEMENT: The authors acknowledge the support from the Faculty of Chemical Engineering and the Faculty of Environmental Engineering, Eskisehir University of Technology, Turkey.

REFERENCES

[1] P. S. Vassileva, I. M. Uzunov and D. K. Voykova, *Cellulose Chem. Technol.*, **56**, 1117 (2022), https://doi.org/10.35812/CelluloseChemTechnol.2022.56.100

[2] G. Crini, E. Lichtfouse, L. D. Wilson and N. M. Crini, *Environ. Chem. Lett.*, **17**, 195 (2019), https://doi.org/10.1007/s10311-018-0786-8

[3] W. Tongpoothorn, M. Sriuttha, P. Homchan, S. Chanthai and C. Ruangviriyachai, *Chem. Eng. Res. Des.*, **89**, 335 (2011), https://doi.org/10.1016/j.cherd.2010.06.012

[4] E. Köseoğlu and C. A. Başar, *Adv. Powder Technol.*, **26**, 811 (2015), https://doi.org/10.1016/j.apt.2015.02.006

[5] R. Dhahri, M. Yilmaz, L. Mechi, A. K. D. Alsukaibi, F. Alimi *et al.*, *Sustainability*, **14**, 3245 (2022), https://doi.org/10.3390/su14063245

[6] X. Niu, C. Liu, L. Lia, X. Han, C. Chang *et al.*, *Water Sci. Technol.*, **85**, 2964 (2022), https://doi.org/10.2166/wst.2022.163

[7] M. J. P. Brito, C. M. Veloso, L. S. Santos, R. C. F. Bonomo and R. C. I Fontan, *Powder Technol.*, **339**, 334 (2018), https://doi.org/10.1016/j.powtec.2018.08.017

[8] A. Regti, A. El Kassimi, R. Laamari and M. El Haddad, *J. Assoc. Arab Univ. Basic Appl. Sci.*, **24**, 1 (2017), https://doi.org/10.1016/j.jaubas.2016.07.005

[9] A. H. Jawada, S. A. Mohammed, M. S. Mastuli and M. F. Abdullah, *Desalin. Water Treat.*, **118**, 342 (2018), https://doi.org/10.5004/dwt.2018.22680

[10] A. F. Ali, A. S. Kovo and S. A. Adetunji, *Encaps. Adsorp. Sci.*, **7**, 95 (2017), https://doi.org/10.4236/jeas.2017.72007

[11] L. Lunchao, X. Bo, D. Yan, H. Xinhong and W. Shurong, *Bioresour. Technol.*, **312**, 123 (2020), https://doi.org/10.1016/j.biortech.2020.123614

[12] Y. Diao, W. P. Walawender and L. T. Fan, *Bioresour. Technol.* **81**, 45 (2002), https://doi.org/10.1016/S0960-8524(01)00100-6

[13] M. J. Prauchner and F. R. Reinoso, *Micropor. Mesopor. Mater.*, **152**, 163 (2012), https://doi.org/10.1016/j.micromeso.2011.11.040

[14] M. Lewoyehu, *J. Anal. Appl. Pyrol.*, **159**, 105 (2021), https://doi.org/10.1016/j.jaap.2021.105279

[15] H. Laksaci, A. Khelifi, M. Trari and A. Addoun, *J. Clean. Prod.*, **147**, 254 (2017), https://doi.org/10.1016/j.jclepro.2017.01.102

[16] M. Salimi, Z. Salehi, H. Heidari and F. Vahabzadeh, *J. Environ. Chem. Eng.*, **9**, 105 (2021), https://doi.org/10.1016/j.jece.2021.105403

[17] P. T. Williams and A. R. Reed, *J. Anal. Appl. Pyrol.*, **71**, 971 (2004), https://doi.org/10.1016/j.jaap.2003.12.007

[18] J. Guo and A. C. Lua, *Mater. Lett.*, **55**, 334 (2002), https://doi.org/10.1016/S0167-577X(02)00388-9

[19] T. Yang and A. C. Lua, *J. Colloid Interface Sci*., **267**, 408 (2003), https://doi.org/10.1016/S0021-9797(03)00689-1
[20] T. Budinova, E. Ekinci, F. Yardim, A. Grimm, E. Björnbom *et al*., *Fuel Process. Technol*., **87**, 899 (2006), https://doi.org/10.1016/j.fuproc.2006.06.005
[21] O. Mahi, K. Khaldi, M. S. Belardja, A. Belmokhtar and A. Benyoucef, *J. Inorg. Organomet. Polym. Mater*., **31**, 2095 (2021), https://doi.org/10.1007/s10904-020-01873-3
[22] M. Ouhammou, L. Lahnine, S. Mghazli, N. Hidar, M. Bouchdoug *et al*., *J. Saudi Soc. Agric. Sci*., **18**, 133 (2019), https://doi.org/10.1016/j.jssas.2017.03.003
[23] M. Choudhary, R. Kumar and S. Neogi, *J. Hazard. Mater*., **392**, 122441 (2020), https://doi.org/10.1016/j.jhazmat.2020.122441
[24] A. Fekaouni, G. Henini and Y. Laidani, *Cellulose Chem. Technol*., **56**, 427 (2022), https://doi.org/10.35812/CelluloseChemTechnol.2022.56.37
[25] O. A. Ekpete, A. C. Marcus and V. Osi, *J. Chem*., **2017**, 1 (2017), https://doi.org/10.1155/2017/8635615
[26] F. Mannai, M. Ammar, J. G. Yanez, E. Elaloui and Y. Moussaoui, *Cellulose*, **23**, 2061 (2016), https://doi.org/10.1007/s10570-016-0899-9
[27] E. A. Varol and A. E. Pütün, *J. Anal. Appl. Pyrol*., **98**, 29 (2012), https://doi.org/10.1016/j.jaap.2012.07.001
[28] M. Jagtoyen and F. Derbyshire, *Carbon*, **36**, 1085 (1998), https://doi.org/10.1016/S0008-6223(98)00082-7
[29] G. Özsin, M. Kılıç, E. A. Varol and A. E. Pütün, *Appl. Water Sci*., **9**, 2 (2019), https://doi.org/10.1007/s13201-019-0942-8
[30] N. You, J. Y. Li, H. T. Fan and H. Shen, *J. Adv. Res*., **15**, 77 (2019), https://doi.org/10.1016/j.jare.2018.09.005
[31] P. S Vassileva, A. K. Detcheva, T. H. Radoykova, I. A. Avramova, K. I. Aleksieva *et al*., *Cellulose Chem. Technol*., **52**, 633 (2018), https://www.cellulosechemtechnol.ro/pdf/CCT7-8(2018)/p.633-643.pdf
[32] O. F. Olorundare, T. A. M. Msagati, R. W. M. Krause, J. O. Okonkwo and B. B. Mamba, *Water Air Soil Pollut*., **225**, 2 (2014), https://doi.org/10.1007/s11270-014-1876-2
[33] M. Benadjemia, L. Millière, L. Reinert, N. Benderdouche and L. Duclaux, *Fuel Process. Technol*. **92**, 1203 (2011), https://doi.org/10.1016/j.fuproc.2011.01.014
[34] Y. S. Al-Degs, M. I. El-Barghouthi, A. H. El-Sheikh and G. M. Walker, *Dyes Pigments*, **77**, 16 (2007), https://doi.org/10.1016/j.dyepig.2007.03.001
[35] P. K. Malik, *Dyes Pigments*, **56**, 239 (2003), https://doi.org/10.1016/S0143-7208(02)00159-6
[36] S. Dawood, T. K. Sen and C. Phan, *Water Air Soil Pollut*., **225**, 2 (2014), https://doi.org/10.1007/s11270-013-1818-4
[37] V. S. Lacerda, J. B. L. Sotelo, A. C. Guimaraes, S. H. Navarro, M. S. B. Ascones *et al*., *J. Environ. Manage*., **155**, 67 (2015), https://doi.org/10.1016/j.jenvman.2015.03.007
[38] T. Santhi, A. L. Prasad and S. Manonmani, *Arab. J. Chem*., **7**, 494 (2014), https://doi.org/10.1016/j.arabjc.2010.11.008
[39] T. Santhi, S. Manonmani and T. Smitha, *J. Hazard. Mater*., **179**, 178 (2010), https://doi.org/10.1016/j.jhazmat.2010.02.076
[40] C. Djilani, R. Zaghdoudi, F. Djazi, B. Bouchekima, A. Lallam *et al*., *J. Taiwan Inst. Chem. Eng*., **53**, 112 (2015), https://doi.org/10.1016/j.jtice.2015.02.025
[41] I. A. W. Tan, B. H. Hameed and A. L. Ahmad, *J. Chem. Eng*., **127**, 111 (2007), https://doi.org/10.1016/j.cej.2006.09.010
[42] L. Junxiong and W. Lan, *Front. Environ. Sci. Eng*., **3**, 320 (2009), https://doi.org/10.1007/s11783-009-0030-7
[43] E. D. Revellame, D. L. Fortela, W. Sharp, R. Hernandez and M. E. Zappi, *Clean. Eng. Technol*., **1**, 100032 (2020), https://doi.org/10.1016/j.clet.2020.100032
[44] Y. Laidani, G. Henini, S. Hanini and A. Fekaouni, *St. Cerc. St. CICBIA*, **20**, 609 (2019)
[45] A. H. Jawad, A. S. Abdulhameed, N. N. Bahrudin, N. N. M. F. Hum, S. N. Surip *et al*., *Water Sci. Technol*., **84**, 1858 (2021), https://doi.org/10.2166/wst.2021.355
[46] X. Chen, *Information*, **6**, 14 (2015), https://doi.org/10.3390/info6010014
[47] T. S. Khayyun and A. H. Mseer, *Appl. Water Sci*., **9**, 2 (2019), https://doi.org/10.1007/s13201-019-1061-2
[48] Q. Hu and Z. Zhang, *J. Mol. Liq*., **277**, 646 (2019), https://doi.org/10.1016/j.molliq.2019.01.005
[49] M. Belhachemi and F. Addoun, *Appl. Water Sci*., **1**, 111 (2011), https://doi.org/10.1007/s13201-011-0014-1
[50] L. Li, F. Liu, X. Jing, P. Ling and A. Li, *Water Res*., **4**, 1177 (2011), https://doi.org/10.1016/j.watres.2010.11.009
[51] F. Gimbert, N. M. Crini, F. Renault, P. M. Badot and G. Crini, *J. Hazard. Mater*., **157**, 34 (2008), https://doi.org/10.1016/j.jhazmat.2007.12.072
[52] R. Saadi, Z. Saadi, R. Fazaeli and N. E. Fard, *Korean J. Chem. Eng*., **32**, 787 (2015), https://doi.org/10.1007/s11814-015-0053-7
[53] R. L. Tseng and F. C. Wu, *J. Taiwan Inst. Chem. Eng*., **40**, 197 (2009), https://doi.org/10.1016/j.jtice.2008.09.002
[54] G. Karaçetin, S. Sivrikaya, M. Imamoğlu, *J. Anal. Appl. Pyrol*., **110**, 270 (2014), https://doi.org/10.1016/j.jaap.2014.09.006
[55] R. A. Aftab, S. Zaidi, A. P. K. Aftab, M. A. Usman, A. Y. Khan *et al*., *Alex. Eng. J*., **71**, 355 (2023), https://doi.org/10.1016/j.aej.2023.03.055

[56] A. Regti, M. R. Laamari, S. E. Stiriba, M. El Haddad, *Int. J. Ind. Chem.*, **8**, 187 (2017), https://doi.org/10.1007/s40090-016-0090-z
[57] G. O. El-Sayed, M. M. Yehia and A. A. Asaad, *Water Resour. Ind.*, **7–8**, 66 (2014), https://doi.org/10.1016/j.wri.2014.10.001
[58] M. A. Usman, R. A. Aftab,·S. Zaidi, S. M. Adnan and R. A. K. Rao, *Int. J. Environ. Sci. Technol.*, **19**, 8351 (2022), https://doi.org/10.1007/s13762-021-03571-0
[59] E. Salehi, S. S. Madaeni and V. Vatanpour, *J. Membr. Sci.*, **389**, 334 (2012), https://doi.org/10.1016/j.memsci.2011.10.045
[60] S. K. Milonjic, *J. Serb. Chem. Soc.*, **72**, 1363 (2007), https://doi.org/10.2298/JSC0712363M
[61] M. K. Purkait, A. Maiti, S. DasGupta and S. De, *J. Hazard. Mater.*, **145**, 287 (2007), https://doi.org/10.1016/j.jhazmat.2006.11.021
[62] M. Danish, R. Hashim, M. N. Mohamad Ibrahim and O. Sulaiman, *Wood Sci. Technol.*, **48**, 1085 (2014), https://doi.org/10.1007/s00226-014-0659-7